The FASEB Journal article fj.09-146357. Published online March 30, 2010.

Proteomic identification of sorting nexin 6 as a negative regulator of BACE1-mediated APP processing

Hirokazu Okada,* Wenzhu Zhang,† Corrinne Peterhoff,§ Jeremy C. Hwang,* Ralph A. Nixon,§ Sung H. Ryu,‖ and Tae-Wan Kim*,†,‡,1

*Integrated Program in Cellular, Molecular, and Biophysical Studies, †Department of Pathology and Cell Biology, and ‡Taub Institute for Research on Alzheimer's Disease and the Aging Brain, Columbia University Medical Center, New York, New York, USA; §Center for Dementia Research, Nathan Kline Institute for Psychiatric Research, Orangeburg, New York, USA; and ‖Department of Life Science and Division of Molecular and Life Sciences, Pohang University of Science and Technology, Pohang, South Korea

ABSTRACT **The β-site APP cleaving enzyme-1 (BACE1) mediates the first cleavage of the β-amyloid precursor protein (APP) to yield the amyloid β-peptide (Aβ), a key pathogenic agent in Alzheimer's disease (AD). Using a proteomic approach based on in-cell chemical cross-linking and tandem affinity purification (TAP), we herein identify sorting nexin 6 (SNX6) as a BACE1-associated protein. SNX6, a PX domain protein, is a putative component of retromer, a multiprotein cargo complex that mediates the retrograde trafficking of the cation-independent mannose-6-phosphate receptor (CI-MPR) and sortilin. RNA interference suppression of SNX6 increased BACE1-dependent secretion of soluble APP (sAPPβ) and cell-associated fragments (C99), resulting in increased Aβ secretion. Furthermore, SNX6 reduction led to elevated steady-state BACE1 levels as well as increased retrograde transport of BACE1 in the endocytic pathway, suggesting that SNX6 modulates the retrograde trafficking and basal levels of BACE1, thereby regulating BACE1-mediated APP processing and Aβ biogenesis. Our study identifies a novel cellular pathway by which SNX6 negatively modulates BACE1-mediated cleavage of APP.—Okada, H., Zhang, W., Peterhoff, C., Hwang, J. C., Nixon, R. A., Ryu, S. H., Kim, T.-W. Proteomic identification of sorting nexin 6 as a negative regulator of BACE1-mediated APP processing. *FASEB J.* 24, 000–000 (2010). www.fasebj.org**

Key Words: protein trafficking · Alzheimer's disease · endosome · trans-Golgi network · retromer

The amyloid β-peptide (Aβ) is the major constituent of amyloid plaques associated with Alzheimer's disease (AD) and is produced by sequential proteolytic cleavage of the amyloid precursor protein (APP) by a set of membrane-bound proteases termed β- and γ-secretases (1). The β-site APP cleaving enzyme-1 (BACE1) cleaves APP to generate 2 proteolytic derivatives, including a secreted APP derivative (sAPPβ) and a membrane-anchored C-terminal fragment (C99; refs. 2–4). Subsequent cleavage of C99 within its transmembrane domain by γ-secretase liberates the C-terminal end of Aβ.

BACE1 is a type I transmembrane protein with a long lumenal ectodomain containing 2 active-site motifs characteristic for aspartyl proteases (DTGS and DSGT) and a short 21-residue cytoplasmic domain. BACE1 is intracellularly transported in the secretory pathway from the endoplasmic reticulum through the trans-Golgi network (TGN) to the cell surface (5). After endocytosis from the plasma membrane to early endosomal compartments, BACE1 is retrogradely recycled back to the TGN or destined to lysosomes for degradation (6–8). The majority of BACE1 is thus localized to Golgi/TGN and endosomal compartments (6). An acidic cluster-dileucine sorting signal (DXXLL) in the cytoplasmic domain of BACE1 has been shown to regulate the endosomal trafficking of BACE1 (9, 10) by either Golgi-localized γ-ear-containing ARF binding proteins (GGAs) or retromers (7, 11–14). For instance, reducing VPS26, a component of the retromer complex by RNA intereference (RNAi) leads to BACE1 accumulation in endosomes, a result similar to that obtained from the reduction of GGAs (7).

Previous studies (5, 15–18) have localized BACE1-mediated cleavage of APP primarily to intracellular membrane compartments, such as endosomes and the TGN, whose lumens have an acidic pH optimal for BACE1 enzymatic activity. As with BACE1, APP is also transported in the secretory pathway and subsequently targeted to the endosomal system. This targeting is a crucial step for the generation of the bulk of Aβ (5, 19, 20). The intracellular trafficking of BACE1 and APP affects the convergence of these 2 molecules and is potentially important in the generation of Aβ. Our

[1] Correspondence: Department of Pathology and Cell Biology, 630 West 168th St., P&S 12-430, New York, NY 10032, USA. E-mail: twk16@columbia.edu

doi: 10.1096/fj.09-146357

previous study (21) revealed that VPS35, another component of the retromer complex, regulated Aβ generation and thus implicated retrograde trafficking in APP processing. Recently, sorting protein-related receptor (SorLA/LR11), a member of the Vps10p family, has been shown to regulate the intracellular trafficking and processing of APP (22, 23). Interestingly, it has also been revealed that SorLA and SorCS1 (another member of the Vps10p family) are genetically associated with late-onset AD (24, 25). These observations suggest that aberrant regulation of certain molecular components in the endocytic retrograde trafficking pathway, including retromers (21) and GGAs (26), may contribute to enhanced amyloidogenesis associated with AD. To this end, we set out to identify molecules that control BACE1 activity in the endosomal trafficking pathway using a unique proteomic approach.

MATERIALS AND METHODS

Plasmids

The C-terminal tandem affinity purification (TAP) tagging cassette was PCR amplified using pBS1479 vector (gift of Cellzome, Heidelberg, Germany) as a template and introduced into pcDNA3.1(+) for mammalian expression using the *Xba*I site. To construct the BACE1-TAP vector, the cDNA sequence corresponding to full-length BACE1 (AF190725) was subcloned into the above-mentioned pcDNA3.1 expressing the C-terminal TAP tag. A missense mutation (D92G) was introduced using the QuikChange site-directed mutagenesis kit (Stratagene, La Jolla, CA, USA) with 5′-CATCCTGGTGGGTACAGGCAG and 5′-CTGCCTGTACCCACCAGGATG primers to generate inactive BACE1 (D92G)-TAP. C-terminal myc-tagged BACE1 was generated by subcloning full-length BACE1 cDNA into pCDNA3.1/Myc-His (Invitrogen, Carlsbad, CA, USA). SNX6 was cloned from HeLa total mRNA using 5′-ATGATGGAAGGCCTGGAC and 5′-TGATGTGTCTCCATTTAACACTGCC primers. The SNX6 full-length construct was subcloned into pEF6-V5His-TOPO (Invitrogen). GenBank sequence was used for verification. Full-length SNX6 cDNA, and 2 SNX6 deletion constructs [ΔBAR: the N-terminal half (aa 1–176) harboring only the PX domain and ΔPX: the C-terminal half (aa 172–406) containing the BAR domains] were also subcloned into pNICE-HA-N (gift of Dr. Peter Scheiffele, University of Basel, Basel, Switzerland).

Cell lines

SH-SY5Y, HEK293, and Neuro2a cells were maintained in DMEM supplemented with 10% FBS and penicillin/streptomycin/glutamine (Invitrogen). For stable transfection, Superfect transfection reagent (Qiagen, Valencia, CA, USA) was used according to the manufacturer's protocol. Stable cell lines were generated by transfecting the cells with the plasmids described above. Antibiotic-resistant colonies were then screened by Western blot.

Antibodies

Polyclonal sβwt antibody was generated by immunizing rabbits with keyhole limpet hemocyanin-conjugated peptides corresponding to the C-terminal region of secreted APPβ, (C)GGGISEVKM. Polyclonal APP-CTmax was previously described (27). Additional immunological reagents include the following: 6E10 to detect C99 and sAPPα (Covance), LN27 to detect APP ectodomain (Invitrogen), monoclonal BACE-Cat1 antibody (gift of Dr. Robert Vassar, Northwestern University, Chicago, IL, USA), polyclonal anti-BACE1 (ProSci Inc., Calbiochem, San Diego, CA, USA), anti-SNX6 (Santa Cruz Biotechnology, Santa Cruz, CA, USA), monoclonal HA (Covance), 9E10 and 9E10 affinity matrix (Covance, Princeton, NJ, USA), anti-V5 (Invitrogen), and organelle-specific antibodies (BD Biosciences, San Jose, CA, USA) except anti-TGN46 (Serotec, Raleigh, NC, USA), anti-Rab7 (Sigma, St. Louis, MO, USA), and anti-LAMP2 (Santa Cruz).

Formaldehyde cross-linking

Formaldehyde cross-linking was performed as described previously (28), with some modifications. SH-SY5Y cells stably expressing BACE1-TAP or BACE1(D92G)-TAP were detached with trypsin-EDTA, washed with PBS, and incubated in 0.5% (wt/vol) paraformaldehyde in PBS for 15 min at 37°C. The cross-linking reaction was stopped by adding 1 M Tris (pH 8.0) to a final concentration 200 mM for 5 min at room temperature. Then cells were washed twice with PBS and lysed with a buffer (50 mM Tris, pH 8.0; 150 mM NaCl; 1% Nonidet P-40; and protein inhibitor mixture). Cell lysates were centrifuged for 10 min at 14,000 rpm. Supernatants were stored at −80°C.

Purification of BACE1 protein complexes

Supernatants of the cross-linked SH-SY5Y cell lysates were thawed, and total protein was quantified using BCA protein assay kit (Pierce, Rockford, IL, USA). To purify the cross-linked BACE1 complexes, the TAP method was used as described previously (29), with some modifications. In brief, 200 mg of cross-linked lysate was centrifuged at 30,000 *g* for 30 min. The supernatant was mixed with 1 ml IgG-Sepharose beads, incubated for 3 h at 4°C, applied onto a chromatography column, and allowed to pack by gravity. After being washed with 30 ml IPP 150 buffer and 10 ml TEV cleavage buffer, the beads were incubated with 500 U TEV in 5 ml TEV cleavage buffer overnight at 4°C. The eluate was then combined with 3 vol of CBB buffer, 3 μl 1 M $CaCl_2$/mg IgG eluate, and 300 μl calmodulin resin, and incubated for 1.5 h at 4°C. The mixture was applied onto a new column. After being washed with 20 ml CBB buffer containing 0.1% Nonidet P-40 and 10 ml CBB buffer containing 0.05% Nonidet P-40, the column was eluted with 1 ml CEB buffer containing 0.05% Nonidet P-40. The eluate was concentrated by centrifugation at 4000 rpm for 20 min at 4°C using an Amicon Ultra-4 10,000 MWCO centrifugal filter device (Millipore, Bedford, MA, USA). To reverse the cross-linking, 4× Tris-glycine sample buffer was added to the concentrated eluate and boiled for 20 min at 95°C. The reversed eluate was resolved by SDS-PAGE on a 4–20% gradient Tris-glycine gel (Invitrogen) and visualized with a GelCode blue stain reagent (Pierce). Bands were excised from the gel for mass spectrometry peptide sequencing.

RNAi

Short-hairpin RNA (shRNA) vectors targeting human SNX6 (and a nonsilencing shRNA vector) were purchased from Sigma. shRNA vectors targeting mouse SNX6 were generated using LentiLox3.7 vectors. The stem loops for the LentiLox3.7 vectors were created following the protocol provided by Tom Tuschl's laboratory website (Rockefeller University, New York, NY, USA; http://www.rockefeller.edu/labheads/tuschl/).

The target sequence selected for mouse SNX6 was 5′-AAGTCGGACAGAATGACAAGATC. Transfection was performed using Superfect (Qiagen) or Lipofectamine 2000 (Invitrogen) according to the manufacturers' protocol.

Soluble APP quantification and Aβ analysis

HEK293 cells stably expressing SNX6-targeting shRNA (or control shRNA) were grown in 6-well dishes and transfected with APP constructs. In other cases, HEK293 and Neuro2a cells stably expressing APP were grown in 6-well dishes and transfected with SNX6 constructs or shRNA vectors. Cell media were collected and subjected to immunoprecipitation with antisera against sAPP and subsequent Western blot analysis with LN27 antibody. Quantification of protein bands was performed using the Odyssey Infrared Imaging System (LI-COR, Lincoln, NE, USA). Quantification of Aβ in cell media was performed using the Aβ ELISA kit (Biosource, Camarillo, CA, USA) according to the manufacturer's protocol.

Immunocytochemistry and immunohistochemistry

HeLa cells were grown in 4-chamber culture slides (BD Biosciences) and transfected. Two days after transfection, cells were washed with PBS and fixed for 15 min with 4% paraformaldehyde in PBS. Then cells were permeabilized for 3 min with 0.1% Triton X-100 in PBS. After being washed with PBS, the cells were incubated for 1 h with blocking solution (10% normal goat serum in PBS) and incubated overnight at 4°C with primary antibodies in a blocking buffer containing 0.1% Triton X-100. After extensive washing, cells were incubated for 1 h with Alexa-labeled secondary antibodies (Molecular Probes, Eugene, OR, USA). The fluorescent signals were visualized with Nikon C1 confocal laser scanning system (Nikon, Melville, NY, USA). To analyze BACE1/SNX6 colocalization, confocal image pixels that showed costaining of BACE1 and SNX6 were determined and assigned a green color using the "colocalization finder" plug-in in ImageJ software (U.S. National Institutes of Health, Bethesda, MD, USA). The green image was then merged with red organelle staining (*e.g.*, TGN46 and EEA1) to determine the degree of the colocalization.

For immunohistochemical analysis, mice were anesthetized and transcardially perfused with 4% paraformaldehyde (pH 7.4). Brains were removed and sectioned at 40 μm on a Leica VT1000 vibratome (Leica Microsystems, Wetzlar, Germany). Immunohistochemistry was performed using standard ABC detection. After endogenous peroxidase activity was quenched by incubation in 0.3% hydrogen peroxide, sections were rinsed, blocked in 20% normal rabbit serum, and incubated overnight at room temperature with primary antibody diluted in 20 mM TBS containing 2% BSA, 1% rabbit serum, and 0.4% Triton X-100. On the second day, following incubation in biotinylated anti-goat secondary, sections were incubated in immunoperoxidase using a standard ABC kit. Sections rinsed and developed using DAB as the chromagen were analyzed on a Zeiss AxioskopII microscope equipped with a Zeiss MRm digital camera. In double immunolabeling analyses, sections were blocked with 20% normal donkey serum and incubated with primary antibody cocktails containing SNX6 (Santa Cruz Biotechnology) and rab5 (Santa Cruz Biotechnology) overnight at room temperature. Sections were incubated with biotinylated anti-sheep secondary for 30 min, rinsed, and incubated in streptavidin-conjugated Alexa488 (Invitrogen) in the dark. After 2 h, anti-rabbit or anti-mouse Alexa568 was added to the streptavidin and incubated for 1 h. Samples were analyzed using a Zeiss510 Meta confocal microscope.

Real-time PCR

HeLa cells were transfected with 200 nM siSNX6s or negative control siRNAs. After 2 d of incubation, total RNA was extracted using the RNeasy mini kit (Qiagen). First-strand cDNA was synthesized with Oligo-dT (20 bases) priming using SuperScript III reverse transcriptase (Invitrogen). The PCR reaction was prepared using LightCycler FastStart DNA MasterPlus SYBR Green I (Roche Applied Science, Indianapolis, IN, USA) in combination with target-specific primers for human BACE1 (5′-CCTTCGTTTGCCCAAGAAAGTG-3′ and 5′-CCCATTAGGTAGAGTGAGATGACTGG-3′), human SNX6 (5′-CCACCAGCACCACCAAGACC-3′ and 5′-TGCCACACGACACAGGAACAC-3′), and human β-actin (5′-GCTCGTCGTCGACAACGGCTC-3′ and 5′-CAAACATGATCTGGGTCATCTTCTC-3′). PCR was carried out in the Smart Cycler System (Cepheid, Sunnyvale, CA, USA), and a comparative computed tomography method was used to quantify BACE1 and SNX6 mRNA levels (normalized to β-actin mRNA).

Sucrose density gradient fractionation

Neuro2a cells stably expressing Swedish variant of APP or HEK293 cells stably expressing BACE1-myc were detached, washed with PBS, and resuspended in sucrose buffer (0.25 M sucrose; 10 mM Tris, pH 7.4;, 2 mM Mg-acetate; 0.5 mM EDTA; and protein inhibitor mixture). Cells were homogenized using a ball-bearing homogenizer, loaded onto a sucrose step gradient [1 ml 0.25 M sucrose, 2 ml 0.5 M sucrose, 2 ml 0.8 M sucrose, 2.5 ml 1.16 M sucrose, 2.5 ml 1.3 M sucrose, and 1.5 ml 2 M sucrose in gradient buffer (10 mM Tris, pH 7.4, and 1 mM Mg-acetate)], and centrifuged at 39,000 rpm for 2.5 h at 4°C with a Beckman SW41Ti rotor (Beckman Instruments, Fullerton, CA). Twelve 1-ml fractions were collected from the top. To analyze the distribution of SNX6, BACE1, APP, and organelle markers, equal volumes were taken from each fraction, separated on a 4–20% gradient Tris-glycine gel, and subjected to Western blot analysis.

Pulse-chase experiment

To perform pulse-chase experiments of BACE1, HaloTag (Promega, Madison, WI, USA) was fused to the C terminus of BACE1. HEK293 cells stably expressing SNX6-targeting shRNA (or control shRNA) were grown in 24-well plates and transfected with BACE1-HaloTag. After 1 d of incubation, BACE1-HaloTag protein was labeled *in vivo* for 15 min with biotin-conjugated HaloTag ligands and, after washing, it was chased to determine its half-life.

Antibody uptake assay

HEK293 cells stably expressing SNX6-targeting shRNA (or control shRNA) grown on polylysine-coated glass coverslips were transfected with BACE1. After 1 d of incubation, cells were washed and incubated for 15 min on ice with ice-cold PBS. Subsequently, the cells were incubated for 30 min on ice with OptiMEM (Gibco-BRL, Gaithersburg, MD, USA) containing an antibody against the ectodomain of BACE1 and, after washing, they were incubated at 37°C in OptiMEM for various time periods. Cells were then fixed with 4% paraformaldehyde and processed for immunocytochemistry. Quantitative analysis of BACE1 subcellular localization was performed by examining the degree of TGN-like perinuclear accumulation in 125 cells/case, on average. Categories used for scoring the degree of the accumulation are little, partial, prominent, and exclusive.

RESULTS

Purification of BACE1-harboring protein complex

To identify proteins that are associated with BACE1, we performed affinity purification of the BACE1-harboring molecular complex. BACE1 has been shown to be present mainly in monomeric form in the presence of detergent (9). To stabilize the BACE1-haboring protein complex and to improve purification efficiency, we employed an in-cell chemical cross-linking and TAP strategy (28, 30). In-cell chemical cross-linking was performed using formaldehyde as the cross-linking reagent at the concentration that introduces specific protein-protein cross-links (29; **Fig. 1*A***). Formaldehyde has several advantages over other popular cross-linkers (*e.g.*, DSP). It is water soluble and nevertheless permeates cell membranes so that it can disperse throughout the cell without vehicles (29). The reaction is also reversible, making it easier to identify the components by mass spectrometry. To efficiently isolate the cross-linked BACE1-harboring complex, BACE1-TAP constructs encoding wild-type BACE1 were introduced into SH-SY5Y human neuroblastoma cells to generate stable transfectants (Fig. 1*B*). The increased levels of C99, a cell-associated APP C-terminal stub derived from BACE1 cleavage, as well as increased generation of secreted sAPPβ and Aβ (data not shown), were observed in SY5Y cells expressing BACE1-TAP, suggesting that TAP-conjugated BACE1 is active (Fig. 1*B*). The stable cells were subjected to formaldehyde cross-linking, which gave rise to a number of high-molecular-weight species that contain BACE1 immunoreactivity, as detected by Western blot analysis (Fig. 1*C*). The purified high-molecular-weight species are mostly smaller than ~300 kDa, suggesting that each species consist of 1 or a few (at most) proteins cross-linked to BACE1. Approximately 200 mg of cross-linked lysate of BACE1-TAP SY5Y cells was prepared and subjected to the published TAP purification process with minor modifications (28, 30; Fig. 1*A*, *C*). The cross-linked

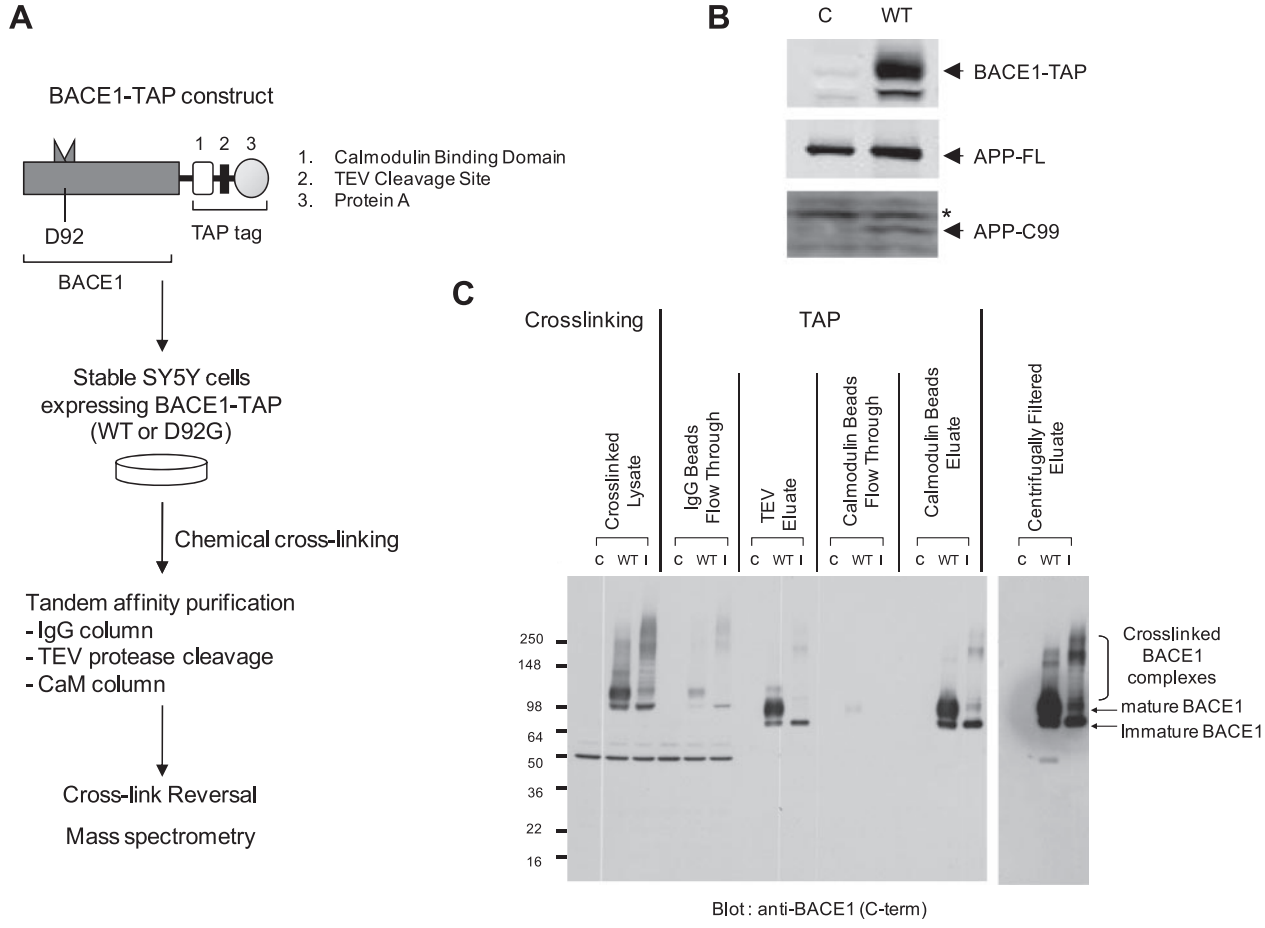

Figure 1. Proteomic identification of SNX6 as a component of BACE1-harboring protein complex. *A*) Schematic representation of BACE1-TAP protein and purification strategy. TAP tag consists of the calmodulin binding domain, TEV protease cleavage site, and protein A, and was fused to the C terminus of BACE1. Inactive BACE1-TAP was generated by introducing a missense mutation (D92G) at the active site. *B*) Western blot analysis of SY5Y cells stably expressing either control vector (C) or BACE1-TAP (WT). Elevated C99 levels were observed in the stable SY5Y cells expressing BACE1-TAP. C99 was detected by 6E10 antibody, and asterisk denotes nonspecific bands. *C*) TAP process of BACE1-harboring complex prepared from formaldehyde (FA)-cross-linked SY5Y cell lysates. Samples from each purification step were analyzed by Western blotting using anti-BACE1 antibody. BACE1-TAP and BACE1 (D92G)-TAP cross-linked to higher molecular complexes.

TABLE 1. *Proteins identified by tandem mass spectrometry*

Putative function	Symbol	Protein	Accession no.
Protease	BACE1	β-Site APP-cleaving enzyme 1	P56817
Protein trafficking	SNX6[a]	Sorting nexin 6	Q9UNH7
	TRAPPC5[a]	Trafficking protein particle complex 5	Q8IUR0
	GDI2[a]	GDP dissociation inhibitor 2 (Rab GDI-β)	P50395
Protein folding	CANX	Calnexin	P27824
	CALR	Calreticulin	P27797
	PDIA3	Protein disulfide isomerase family A, member 3	P30101
	TXNDC1	Thioredoxin domain containing 1	Q9H3N1
	HSPA5	Heat-shock 70-kDa protein 5	P11021
	PPIB	Peptidylprolyl isomerase B (cyclophilin B)	P23284
	PPIA	Peptidylprolyl isomerase A (cyclophilin A)	P62937
Others	P4HB	Procollagen-proline, 2-oxoglutarate 4-dioxygenase (proline 4-hydroxylase), β-polypeptide	P07237
	ATP5A1	ATP synthase, H^+ transporting, mitochondrial F1 complex, α-subunit 1	P25705
	SLC25A5	Solute carrier family 25 (mitochondrial carrier; adenine nucleotide translocator), member 5	P05141
	TUBA1A[a]	Tubulin, α-1a	Q71U36
	TUBB4Q[a]	Tubulin, β-polypeptide 4, member Q	Q99867
	MYLK2	Myosin light chain kinase 2	Q9H1R3

[a]Protein that is present only in the wild-type BACE1-TAP complex and not in the D92G BACE1-TAP.

BACE1 complex was not readily visible in TEV and calmodulin bead eluates because cross-linked samples had to be diluted to neutralize the reaction before the subsequent chromatographic steps. After the reconcentration step, high-molecular-weight complexes were readily detectable (Fig. 1*C*). Our multistep process identified 16 proteins as putative components of the BACE1 molecular complex (**Table 1**). Five proteins were identified in the wild-type (active) BACE1 complex but not in the D92G (inactive) BACE1 complex, including sorting nexin 6 (SNX6), trafficking protein particle complex 5 (TRAPPC5), and GDP association inhibitor 2 (GDI2; Table 1).

Identification of SNX6 as a component of the BACE1 complex

The peptide sequences obtained from the identifiable ~60-kDa band corresponded to those of human SNX6 (**Fig. 2*A***). Since our interest was to search for cellular modulators of BACE1 activity and intracellular traffick-

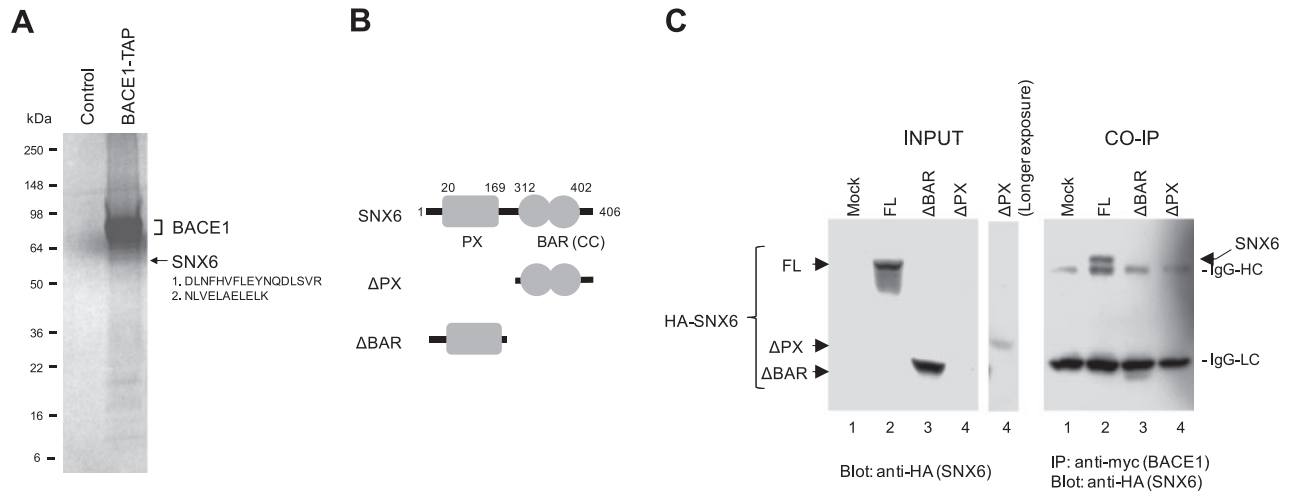

Figure 2. Identification of SNX6 as a BACE1-interacting protein. *A*) Coomassie staining of the components of BACE1-harboring protein complexes from a control line and a cell line stably expressing BACE1-TAP. Bands were excised from the gel and analyzed by mass spectrometry. Band and peptide sequences corresponding to SNX6 are shown. *B*) Schematic representation of SNX6 protein containing PX and BAR (CC) domains and 2 deletion constructs (ΔPX and ΔBAR). Amino acid numbers are shown. *C*) Coimmunoprecipitation (CO-IP) of SNX6 with BACE1. Cross-linked lysates prepared from HeLa cells expressing mock (lane 1), HA-tagged SNX6 (lane 2; FL), ΔPX (lane 3), and ΔBAR (lane 4) were subjected to the immunoprecipitation using anti-myc antibodies to pull down BACE1. After reversal of cross-linking, ~60-kDa HA-SNX6 was detected by anti-HA antibody. IgG-HC and IgG-LC denote immunoglobulin heavy- and light-chain bands, respectively.

ing, we first set out to characterize SNX6, a member of the sorting nexin (SNX) family that is characterized by the presence of a PX (Phox homology) domain at its N terminus and a BAR (Bin/amphiphysin/Rvc) domain at its carboxyl region (Fig. 2*B*). Sorting nexins have been implicated in various functions, including endosomal sorting, recycling, internalization, and prodegradative sorting (31–34). Interestingly, SNX6 has been suggested as a component of retromer, which mediates the retrograde trafficking of select membrane cargo from endosomes to the TGN (35). Defects in retromer in AD brains have been implicated in earlier studies (21).

To confirm the interaction between BACE1 and SNX6, HeLa cells were transiently transfected with HA-SNX6 and BACE1-myc and subjected to chemical cross-linking followed by coimmunoprecipitation. The BACE1-SNX6 complex was pulled down by anti-myc beads, and the ~60-kDa SNX6-V5 was liberated from the complex after reversal of cross-linking (Fig. 2*C*). The SNX6-BACE1 interaction was detergent-sensitive, since the BACE1-SNX6 complex was not detectable when using ionic or nonionic detergents in the absence of cross-linking (data not shown). When the BAR domain was deleted, SNX6 failed to form a complex with BACE1, indicating that the BAR domain may be obligatory for the formation of BACE1-SNX6 complex (Fig. 2*B*, *C*). For ΔPX constructs, we were not able to express ΔPX protein in readily detectable levels, suggesting that the ΔPX domain is required for the stability of SNX6. Our data suggest that both the PX and BAR domains are required for the proper interaction with BACE1. Thus, we have confirmed the interaction of SNX6 with BACE1, indicating that our purification strategy allows for detection of the detergent-sensitive interaction between BACE1 and SNX6.

Colocalization of SNX6 with BACE1 in the vesicular structures near theTGN

We next performed confocal microscopy to determine the subcellular compartments that SNX6 and BACE1 localize to in HeLa cells. As previously reported (25), SNX6 showed a punctate staining pattern reminiscent of endosomal structures with substantial costaining with an early endosomal marker, EEA (Supplemental Fig. 1*A*). Since BACE1 is known to localize in the TGN in addition to the endosomes (6–9, 13), we next performed triple color staining for BACE1 and SNX6 along with an organelle marker (*e.g.*, TGN46 or EEA1) to determine the subcellular sites where the SNX6 and BACE1 immunoreactivity colocalize. We found that colocalization of SNX6 and BACE1 occurs in neighboring vesicles around the TGN46-positive structure (Supplemental Fig. 1*B*). Further colocalization analysis revealed that SNX6 and BACE1 colocalization was predominantly restricted to the vesicular structures in proximity to the TGN and virtually absent in the TGN46-positive TGN (Supplemental Fig. 1*C*). Since SNX6 exhibited substantial colocalization with EEA1, a marker for early endosomes, we next used the same image analysis technique to determine whether SNX6 and BACE1 colocalization occurs in the EEA1-positive vesicles. We found that puncta that are positive for BACE1 and SNX6 are rare and far less prominent in the EEA1-positive vesicles (data not shown). Our data suggest that the subcellular sites for the BACE1 and SNX6 interaction are the vesicular structures near the TGN.

Expression of SNX6 in neurons of the mammalian brain

Since cellular distribution of SNX6 in the mammalian brain has not been previously demonstrated, we next performed immunohistochemical analyses in brain tissue of C57BL/6 mice to determine whether SNX6 can be detected in the neuronal populations implicated in AD. We found that SNX6 is principally localized to neurons (**Fig. 3*A***) and is concentrated within perikarya and proximal dendrites (Fig. 3*B*, *C*, *F*). SNX6 distributed widely, but nonuniformly, throughout the brain and was most abundant in the neocortex (Fig. 3*B*, *C*), entorhinal cortex (Fig. 3*D*), subiculum (Fig. 3*E*), and specific subcortical neuronal populations, notably the medial septal nucleus (Fig. 3*F*). Hippocampal labeling, while relatively weak, was evident in dendrites of CA1 pyramidal neurons (Fig. 3*G*). Consistent with localization studies in HeLa cells (data not shown), SNX6 exhibited a punctate cellular staining pattern, which coincided with rab 5-positive organelles in double immunofluorescence analyses (Fig. 3*H–J*).

SNX6 modulates BACE1-mediated cleavage of APP

To evaluate the potential role of SNX6 in BACE1 function, we first examined whether reducing SNX6 levels affects BACE1-mediated cleavage of APP. SNX6-knockdown cells were generated by stably transfecting HEK293 cells with SNX6-directed shRNA. SNX6 protein levels were substantially reduced in the SNX6 shRNA-expressing stable clonal lines compared with cells expressing control shRNA (**Fig. 4*A***). BACE1 cleaves APP to generate 2 major proteolytic derivatives, including a secreted APP ectodomain (sAPPβ) and a membrane-anchored C-terminal fragment (C99). To analyze the secreted APP derivatives in SNX6-reduced cells, conditioned media were subjected to immunoprecipitation using either the sAPPβ-specific antibody (sβwt) or the α-secretase-derived secreted APP (sAPPα)-reactive 6E10 antibody, followed by infrared-based quantitative Western blot analysis using LN27, which recognizes the N-terminal portion of APP (Fig. 4*B*). Secretion of sAPPβ was significantly elevated in SNX6-knockdown cells compared with controls (Fig. 4*B*, *C*). In contrast, levels of α-secretase-derived sAPPα were not affected by SNX6 reduction (Fig. 4*D*). Similar results were obtained when SNX6 shRNAs were transiently introduced in HEK293 cells or Neuro2a cells (data not shown). Interestingly, the increase in sAPPβ correlated well with

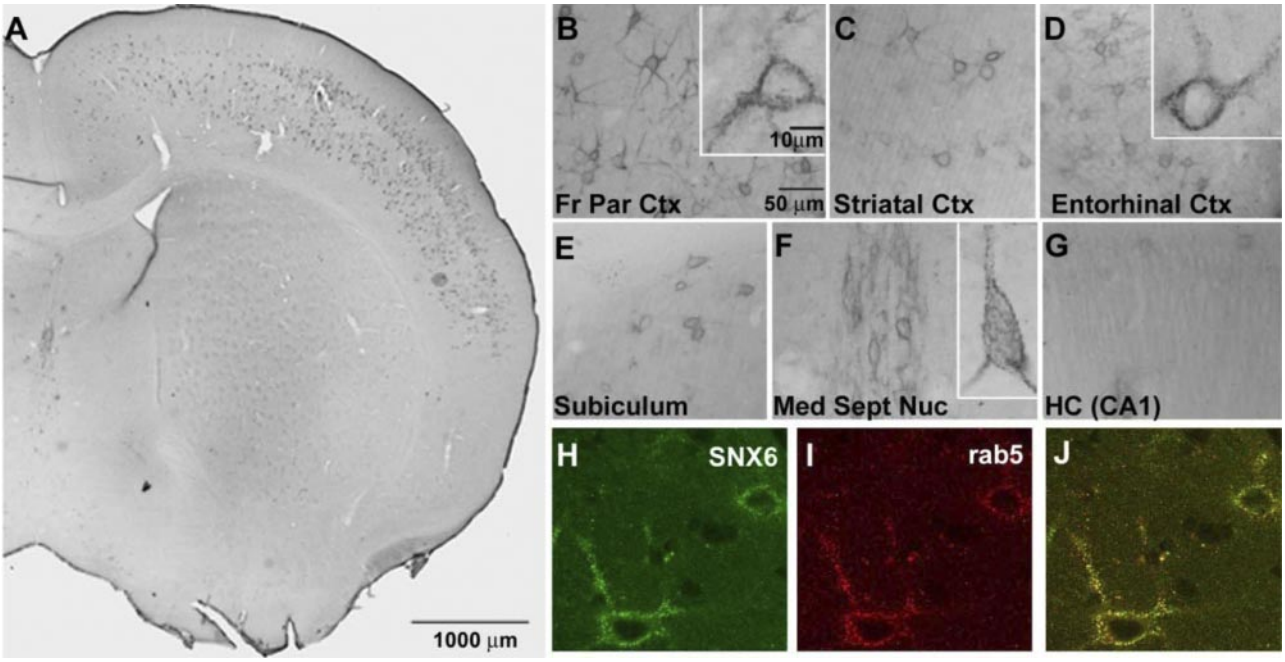

Figure 3. SNX6 expression in mouse brain. *A*) Immunohistochemical analyses in brain tissue of C57Bl/6 mice show neuronal distribution in the cortical layers. *B–G*) Regional distribution of SNX6 in mouse brain: front parietal cortex (*B*), striatal cortex (*C*), entorhinal cortex (*D*), subiculum (*E*), medial septal nucleus (*F*), and hippocampus (*G*; CA). *H–J*) Subcellular colocalization with Rab5: SNX6 (*H*), Rab5 (*I*), and overlay (*J*). Note the predominant neuronal expression of SNX6 in indicated regions of the mouse brain.

the magnitude of SNX6 reduction in cells transfected with varying levels of SNX6 overexpression constructs or SNX6 shRNA (Supplemental Fig. 2).

Consistent with the observed changes in sAPPβ levels, the β-secretase-derived, membrane-associated C-terminal APP fragments (βCTFs) were also influenced by SNX6 reduction. The levels of the major βCTFs (C99; ref. 36) were significantly elevated in SNX6-knockdown cells compared with controls, whereas the α-secretase-derived C-terminal APP fragment (C83) remained unchanged (Fig. 4*E–G*). Aβ40 generation was also significantly increased in SNX6-knockdown cells as compared with controls (Fig. 4*H*), indicating that increased BACE1 cleavage of APP is likely to lead to the enhanced generation of Aβ. Our data indicate that reducing SNX6 greatly potentiates BACE1-mediated cleavage of APP without influencing α-secretase cleavage of APP.

Since SNX6 levels closely correlate with sAPPβ secretion and C99 levels, we next examined the effect of SNX6 overexpression on BACE1 cleavage of APP and subsequent generation of Aβ. Overexpression of constructs encoding an N-terminal HA epitope-tagged version of SNX6 resulted in reduced secretion of sAPPβ and Aβ (Supplemental Fig. 3*A*, *B*, *D*). Similar effects on Aβ were observed when a non-tagged version of SNX6 was introduced (data not shown). SNX6 overexpression did not influence the secretion of sAPPα (Supplemental Fig. 3*C*). We noticed that transfected SNX6 never reached very high levels. We suspect that there is a certain regulatory mechanism present to tightly control the cellular levels of SNX6. Nevertheless, given the relatively minor increase in the levels of SNX6 in our experiments, we have consistently observed the effects of SNX6 expression on sAPPβ and Aβ. Together with our RNAi data, our results further indicate that sAPPβ levels inversely correlate with the cellular levels of SNX6.

SNX6 modulates the steady-state levels of endogenous BACE1 in neuronal cells

Having established that SNX6 regulates BACE1-mediated APP cleavage, we next set out to investigate the underlying mechanism of this regulation. We first examined whether SNX6 levels affect the cellular protein levels of BACE1. Using Neuro2a cells that were treated with either control or SNX6 RNAi, we performed quantitative Western blot analysis to determine the steady-state levels of endogenous BACE1 in SNX6-knockdown cells (**Fig. 5*A***). Endogenous BACE1 levels were significantly elevated in the cells with reduced SNX6 as compared with control cells (Fig. 5*A*, *B*). To assess whether the increase in BACE1 levels is due to transcriptional up-regulation of BACE1, we performed real-time PCR analyses of BACE1 mRNA in SNX6-knockdown cells. Reduction of SNX6 was achieved using 2 distinct siRNA (together with 2 separate control siRNA), and BACE1 mRNA was quantified and normalized to β-actin mRNA (Fig. 5*C*). While BACE1 protein levels were substantially reduced in SNX6 RNAi cells, BACE1 mRNA levels did not change through modulation of SNX6 levels, indicating that SNX6 modulates

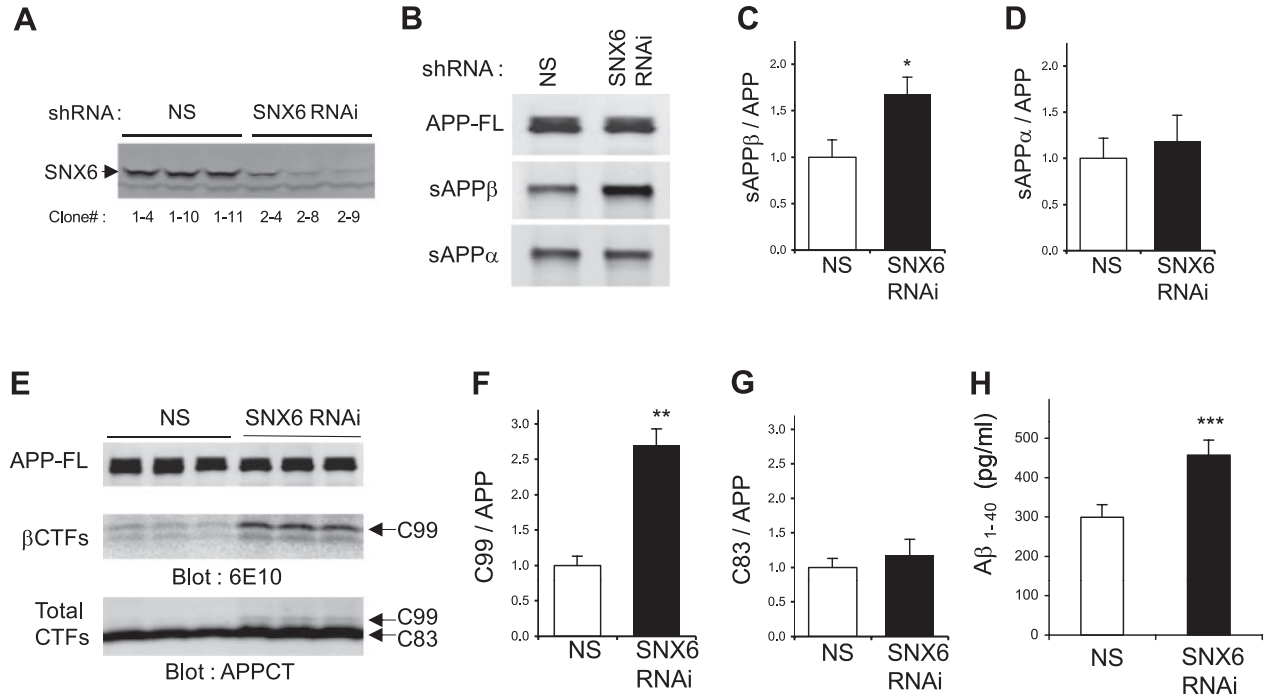

Figure 4. Reducing SNX6 increases BACE1-mediated cleavage of APP. *A*) SNX6 expression in stable HEK293 clonal cell lines transfected with either nonsilencing shRNA vector (NS) or shRNA against human SNX6 (SNX6). *B*) Immunoprecipitation and Western blot analysis of sAPPβ and sAPPα, secreted from the HEK293 stable cells in *A* that were transfected with APP. At 1 d post-transfection, conditioned medium collected after 3 h of incubation was subjected to immunoprecipitation using either BACE1 cleavage site-specific antibody (sβwt) or 6E10, followed by Western blot analysis with LN27 to detect sAPPβ and sAPPα, respectively. *C, D*) Quantification of the sAPPβ (*C*) and sAPPα (*D*) bands (normalized to full-length APP) was performed using infrared-based quantitation (LI-COR) and combining >6 independent experiments. *E*) Detection of a major BACE1-derived C-terminal fragment (C99) and α-secretase-derived C83. HEK293 stable cells in *A* were transfected with APP. After 1 d of incubation with compound E to inhibit γ-secretase activity, cell lysates were subjected to Western blot analyses using indicated antibodies. *F, G*) Quantification of the C99 (*F*) and C83 (*G*) bands (normalized to full-length APP) was performed using infrared-based Western blot analysis (LI-COR) and combining 4 independent experiments. *H*) Reducing SNX6 increases the secretion of $A\beta_{1-40}$. Conditioned medium was subjected to sandwich ELISA to quantify $A\beta_{1-40}$ (n=3). Values are means ± SD. $^*P < 0.0005$, $^{**}P < 0.00005$, $^{***}P < 0.005$; 2-tailed t test.

cellular BACE1 levels post-transcriptionally. Similar results (increased BACE1 levels in SNX6-knockdown cells) were obtained in 293 cells stably expressing BACE1 (data not shown).

Given the effects of SNX6 overexpression on sAPPβ and Aβ (Supplemental Fig. 3), we next examined the steady-state levels of BACE1 in cells expressing increased levels of SNX6. We found that BACE1 was concentrated in the TGN-like fractions in biochemical subcellular fractions (see Materials and Methods) and that BACE1 levels were decreased in the SNX6-overexpressing cells when normalized to syntaxin 6 (Supplemental Fig. 4).

SNX6 does not affect the turnover of BACE1

To explore the possibility that SNX6 regulates the steady-state levels of BACE1 *via* controlling the degradation, we performed pulse-chase experiments to determine the effects of SNX6 reduction on the BACE1 half-life. We first expressed Halo-tagged BACE1 (BACE1-Halo), which allows the covalent modification of the target protein in intact cells, in HEK293 cell lines stably expressing SNX6-targeting shRNA or nonsilencing shRNA. BACE1-Halo expressed in the cells was labeled with biotin-conjugated Halo-tag ligands, chased up to 24 h, and subjected to Western blot analysis of the lysates blotted with streptavidin-conjugated infrared dyes. We found that the turnover rate of BACE1 was not altered in the SNX6-knockdown cells as compared with nonsilencing control cells (Fig. 5*D, E*). Our result indicates that SNX6 does not affect the degradation of BACE1.

SNX6 negatively regulates the retrograde transport of BACE1

Since SNX6 has a putative function in retrograde protein trafficking (35, 37), we hypothesized that SNX6 may influence β-secretase cleavage of APP and cause increased accumulation of BACE1 by influencing the rate of retrograde transport of BACE1. To this end, we investigated whether SNX6 is involved with the retrograde transport of BACE1 from the cell surface through the endosomal structures to the perinuclear structure, including TGN. Using SNX6-knockdown cells and control cells, we first measured the kinetics of BACE1 transport from the cell surface to the perinu-

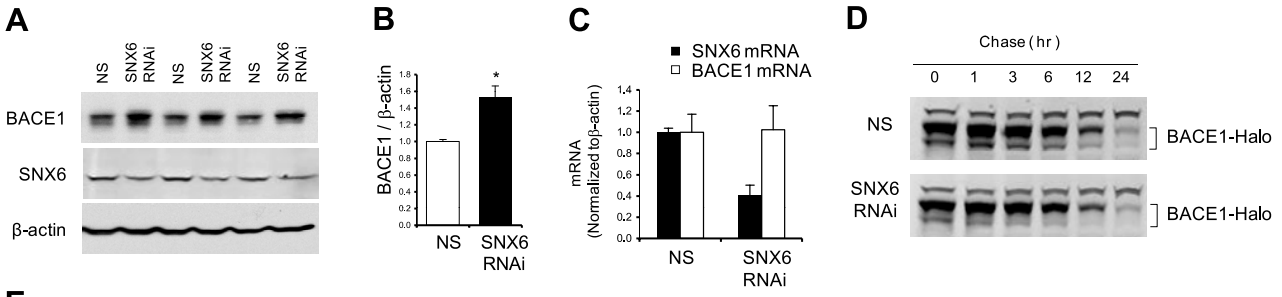

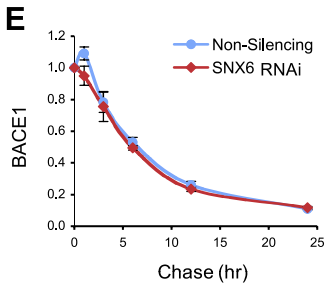

Figure 5. Reducing SNX6 increases basal BACE1 levels. *A*) Reducing SNX6 increases endogenous BACE1 levels. Neuro2a cells stably expressing the Swedish variant of APP were transfected with either nonsilencing shRNA vector (NS) or shRNA against mouse SNX6 (SNX6). After 2 d incubation, cell lysates were subjected to Western blot analysis. *B*) Quantification of BACE1 was performed using NIH ImageJ (n=3). Values are means ± SD. *$P < 0.005$; 2-tailed t test. *C*) Reducing SNX6 does not affect BACE1 mRNA levels. HeLa cells were transfected with 2 distinct SNX6 shRNAs (SNX6 RNAi) or negative control shRNAs (NS). Real-time PCR was performed, and mRNA levels of SNX6 and BACE1, normalized to β-actin mRNA, were quantified. *D*) Pulse-chase experiments using Halo-tagged BACE1. HEK293 cell lines stably expressing either nonsilencing shRNA vector (NS) or shRNA against human SNX6 (SNX6; see Fig. 4*A*) were transfected with Halo-tagged BACE1. After 1 d of incubation, cells were labeled with biotin-conjugated Halo-tag ligand and chased for indicated times. BACE1 turnover was analyzed with Western blot analysis. Representative blots are shown. *E*) Protein levels of BACE1 were plotted with the chased times. Error bars = SD from 3 experiments.

clear vesicles. To monitor the retrograde transport of BACE1, we labeled the cell surface BACE1 with an antibody against the ectodomain of BACE1 and monitored the uptake of antibody-conjugated BACE1 at different time points. At time zero, BACE1 was detected at the cell surface (**Fig. 6*A***). After 8 min of internalization, BACE1 was mostly detected in peripheral vesicles, typical for early endosomal structures in both SNX6-knockdown cells and control cells (Fig. 6*A*). At 18 min, while BACE1 in control cells remained predominantly in peripheral vesicles reminiscent of endosomes, BACE1 in SNX6-knockdown cells showed a significant

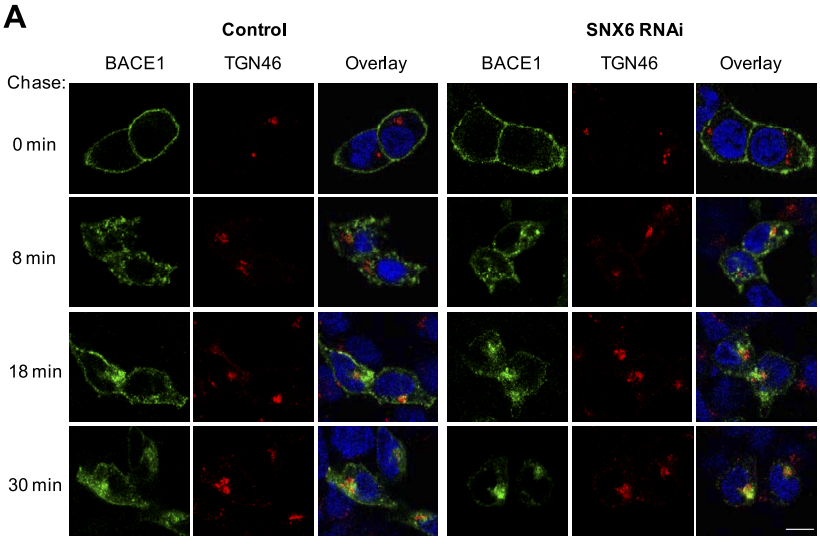

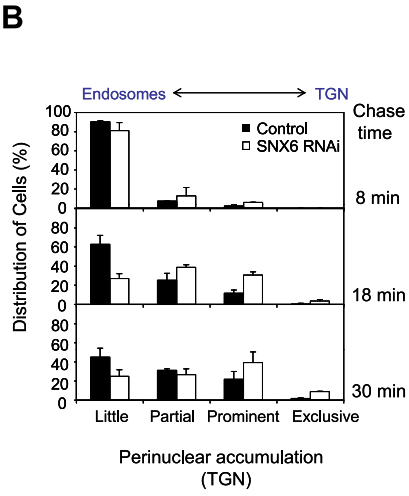

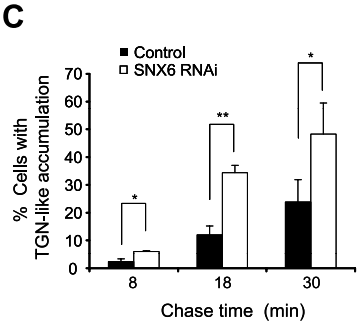

Figure 6. SNX6 negatively regulates the retrograde transport of BACE1. *A*) BACE1 antibody uptake assay was performed using the cell lines used in Fig. 2*A*. Cells were transfected with BACE1. After 1 d of incubation, BACE1 at the cell surface was labeled with anti-BACE1 (N-terminal) antibody and subsequently chased for indicated time periods. Representative confocal images are shown. Scale bar = 10 μm. *B*) Quantitative analysis of BACE1 subcellular localization; 125 cells/case, on average, were examined for degree of perinuclear accumulation near the TGN. Categories used for scoring degree of accumulation: little, partial, prominent, and exclusive. *C*) Percentages of cells that showed dominant perinuclear accumulation (=prominent+exclusive) were plotted at each chase time (n=3). Values are means ± SD. *$P < 0.05$, **$P < 0.001$; 2-tailed t test.

degree of accumulation in a perinuclear structure. At 30 min, BACE1 in SNX6-knockdown cells revealed a predominant localization in the organelles that are adjacent to the TGN46-positive organelle (Fig. 6*A*). The staining of BACE1, however, did not overlap completely with that of TGN46. At the same time, we did not observe any gross morphological disruption of the TGN in SNX6-suppressed cells. At 40 min or longer, the signal starts to fade and BACE1 antibody immunoreactivity show diffused cytoplasmic staining eventually, indicating either dissociation and diffusion of antibodies or degradation of the antibody-BACE1 complex (data not shown). The cell surface-derived BACE1-antibody complex was not detected in other organelles positive for GM130 (cis-Golgi), calnexin (endoplasmic reticulum), EEA1 (early endosomes), Rab11 (recycling endosomes), Rab7 (late endosome), and LAMP2 (lysosome; Supplemental Fig. 5). Thus, the perinuclear structures in which BACE1 accumulates may represent a novel or transient structure located in proximity to the TGN that is not positive for the various subcellular markers we tested. Our data suggest that BACE1 derived from the cell surface undergoes retrograde trafficking and accumulates in focal perinuclear structures in proximity to the TGN marker protein (TGN46). Quantitative comparison between SNX6-knockdown and control cells revealed that reducing SNX6 leads to the increased localization of BACE1 to the TGN-like structure after 18–30 min on internalization (Fig. 6*B, C*), indicating the facilitation of retrograde trafficking of BACE1 from endosomes to the focal perinuclear structures in SNX6-knockdown cells. Thus, our results suggest that SNX6 serves as a negative modulator of BACE1 transport from endosomal compartments to the TGN and novel structures adjacent to the TGN.

DISCUSSION

In this study, we undertook a proteomic approach based on in-cell chemical cross-linking and TAP to identify SNX6 as a component of BACE1 protein complex. We showed that reducing SNX6 *via* RNAi increases the BACE1-derived APP cleavage fragments, including sAPPβ, C89, C99, and $A\beta_{40}$. SNX6 RNAi also increased steady-state cellular BACE1 levels *via* a post-transcriptional mechanism. Our time-lapse imaging studies also indicated a role for SNX6 in controlling the retrograde endocytic transport of BACE1 from the endosome to novel perinuclear focal structures near the TGN.

SNX6 is a member of the PX domain-containing trafficking molecule family that has been shown to play critical roles in membrane trafficking (31–33). One of the suggested functions of SNXs is to assist in the formation of the cargo complex by coincidently detecting specific lipids (*e.g.*, phosphoinositides) and the membrane curvature uniquely present in the donor membrane *via* its PX and BAR domains (31–33, 35, 37). According to our results, the proposed function of SNX6 is opposite that of SNX1, which is a well-characterized component of the retromer complex and known to promote retromer-mediated trafficking of the CI-MPR (cation-independent mannose-6-phosphate receptor; ref. 38). For instance, suppression of SNX1 leads to the redistribution of CI-MPR to endosomes and decreased steady-state levels of CI-MPR (38). However, considering that SNX6 has been shown to bind SNX1 (35, 39), SNX6 may interact with the retromer complex to regulate BACE1 retrograde transport. It is conceivable that SNX6 may antagonize SNX1 function by forming an SNX1-SNX6 complex that favors retention rather than retrograde transport. Alternatively, the SNX6-harboring retromer may have different cargo selectivity compared with the SNX1-bearing retromer complex. Collectively, these data suggest that the role of SNXs is to tightly control the levels of their select target cargo proteins in a given organelle. In the case of both SNX1 and SNX6, SNX-mediated regulation of the steady-state protein levels is attributed to controlling the outflow trafficking of target cargo proteins from the donor membrane.

We have previously shown that the retrograde trafficking pathway involving an adaptor protein complex contributes to the amyloidogenic processing of APP (21). Furthermore, several components that are known to mediate cargo-specific endocytic trafficking (*e.g.*, sorLA and GGAs) were shown to bind APP and BACE1 and influence APP processing (11, 13, 22, 23, 26, 40, 41). GGAs also bind to SorLA/LR11, another member of the Vps10p family of receptors (42). It has recently been shown that SorLA interacts with APP and regulates the intracellular transport and processing of APP (22, 23, 41). Furthermore, the inherited variants in SorLA and SorCS1 (a third member of the Vps10p family) are associated with late-onset AD (24, 25). Recent studies (34, 43) also revealed that at least 2 sorting nexins are found to regulate APP trafficking and ectodomain shedding, suggesting that various sorting nexins may contribute to different aspects of protein trafficking of APP and/or BACE1. BACE1 has recently been shown to interact with GGA (11, 13). Interaction of GGA with the cytoplasmic region of BACE1 was shown to facilitate the retrograde trafficking of BACE1 from endosome to TGN. Since SNX6 reduction enhances retrograde trafficking of BACE1 from endosome to a TGN-like structure, it is conceivable that SNX6 may mediate the BACE1 trafficking pathway opposing to that mediated by GGA. Thus, SNX6 may represent a negative modulator for the endosome to TGN trafficking of BACE1, while GGA serves as a positive modulator for the pathway.

Recent studies (44–48) have demonstrated that BACE1 levels are up-regulated in the brains of AD mouse models as well as AD patients. Furthermore, elevated BACE1 levels appear to increase amyloidogenesis and the risk of developing AD associated with the ischemic brain injuries (47). Immunohistochemical analyses of mouse brains indicated that SNX6 is expressed in neurons of the brain regions known to be vulnerable in AD (Fig. 3). Thus, SNX6-mediated regulation of the steady-state levels of BACE1 and a subsequent increase in the

BACE1-mediated cleavage may be relevant to AD progression. Regulating the activity of BACE1 to reduce the production of Aβ remains a promising strategy for therapeutic intervention in AD (49). Thus, inhibition of BACE1 activity by perturbing other aspects of BACE1 cell biology, such as SNX6, may be envisioned as an alternative strategy in developing AD therapeutics. FJ

This study was supported by an Alzheimer's Disease Research Center grant from the U.S. National Institutes of Health (AG-09702) and by the American Health Assistance Foundation to T.-W.K. The authors thank G. Finan for critical reading of the manuscript, I. S. Kim for technical assistance with molecular biology, and A. Zenobia Moore for assistance with cell culture.

REFERENCES

1. Tanzi, R. E., and Bertram, L. (2005) Twenty years of the Alzheimer's disease amyloid hypothesis: a genetic perspective. *Cell* **120,** 545–555
2. Vassar, R., Bennett, B. D., Babu-Khan, S., Kahn, S., Mendiaz, E. A., Denis, P., Teplow, D. B., Ross, S., Amarante, P., Loeloff, R., Luo, Y., Fisher, S., Fuller, J., Edenson, S., Lile, J., Jarosinski, M. A., Biere, A. L., Curran, E., Burgess, T., Louis, J. C., Collins, F., Treanor, J., Rogers, G., and Citron, M. (1999) Beta-secretase cleavage of Alzheimer's amyloid precursor protein by the transmembrane aspartic protease BACE. *Science* **286,** 735–741
3. Sinha, S., Anderson, J. P., Barbour, R., Basi, G. S., Caccavello, R., Davis, D., Doan, M., Dovey, H. F., Frigon, N., Hong, J., Jacobson-Croak, K., Jewett, N., Keim, P., Knops, J., Lieberburg, I., Power, M., Tan, H., Tatsuno, G., Tung, J., Schenk, D., Seubert, P., Suomensaari, S. M., Wang, S., Walker, D., Zhao, J., McConlogue, L., and John, V. (1999) Purification and cloning of amyloid precursor protein beta-secretase from human brain. *Nature* **402,** 537–540
4. Yan, R., Bienkowski, M. J., Shuck, M. E., Miao, H., Tory, M. C., Pauley, A. M., Brashier, J. R., Stratman, N. C., Mathews, W. R., Buhl, A. E., Carter, D. B., Tomasselli, A. G., Parodi, L. A., Heinrikson, R. L., and Gurney, M. E. (1999) Membrane-anchored aspartyl protease with Alzheimer's disease beta-secretase activity. *Nature* **402,** 533–537
5. Huse, J. T., and Doms, R. W. (2001) Neurotoxic traffic: uncovering the mechanics of amyloid production in Alzheimer's disease. *Traffic* **2,** 75–81
6. Walter, J., Fluhrer, R., Hartung, B., Willem, M., Kaether, C., Capell, A., Lammich, S., Multhaup, G., and Haass, C. (2001) Phosphorylation regulates intracellular trafficking of beta-secretase. *J. Biol. Chem.* **276,** 14634–14641
7. He, X., Li, F., Chang, W. P., and Tang, J. (2005) GGA proteins mediate the recycling pathway of memapsin 2 (BACE). *J. Biol. Chem.* **280,** 11696–11703
8. Koh, Y. H., von Arnim, C. A., Hyman, B. T., Tanzi, R. E., and Tesco, G. (2005) BACE is degraded via the lysosomal pathway. *J. Biol. Chem.* **280,** 32499–32504
9. Huse, J. T., Pijak, D. S., Leslie, G. J., Lee, V. M., and Doms, R. W. (2000) Maturation and endosomal targeting of beta-site amyloid precursor protein-cleaving enzyme. The Alzheimer's disease beta-secretase. *J. Biol. Chem.* **275,** 33729–33737
10. He, X., Chang, W. P., Koelsch, G., and Tang, J. (2002) Memapsin 2 (beta-secretase) cytosolic domain binds to the VHS domains of GGA1 and GGA2: implications on the endocytosis mechanism of memapsin 2. *FEBS Lett.* **524,** 183–187
11. He, X., Zhu, G., Koelsch, G., Rodgers, K. K., Zhang, X. C., and Tang, J. (2003) Biochemical and structural characterization of the interaction of memapsin 2 (beta-secretase) cytosolic domain with the VHS domain of GGA proteins. *Biochemistry* **42,** 12174–12180
12. Bonifacino, J. S. (2004) The GGA proteins: adaptors on the move. *Nature Rev.* **5,** 23–32
13. Wahle, T., Prager, K., Raffler, N., Haass, C., Famulok, M., and Walter, J. (2005) GGA proteins regulate retrograde transport of BACE1 from endosomes to the trans-Golgi network. *Mol. Cell. Neurosci.* **29,** 453–461
14. Seaman, M. N. (2005) Recycle your receptors with retromer. *Trends Cell Biol.* **15,** 68–75
15. Huse, J. T., Liu, K., Pijak, D. S., Carlin, D., Lee, V. M., and Doms, R. W. (2002) Beta-secretase processing in the trans-Golgi network preferentially generates truncated amyloid species that accumulate in Alzheimer's disease brain. *J. Biol. Chem.* **277,** 16278–16284
16. Vassar, R. (2004) BACE1: the beta-secretase enzyme in Alzheimer's disease. *J. Mol. Neurosci.* **23,** 105–114
17. Rajendran, L., Honsho, M., Zahn, T. R., Keller, P., Geiger, K. D., Verkade, P., and Simons, K. (2006) Alzheimer's disease beta-amyloid peptides are released in association with exosomes. *Proc. Natl. Acad. Sci. U. S. A.* **103,** 11172–11177
18. Schneider, A., Rajendran, L., Honsho, M., Gralle, M., Donnert, G., Wouters, F., Hell, S. W., and Simons, M. (2008) Flotillin-dependent clustering of the amyloid precursor protein regulates its endocytosis and amyloidogenic processing in neurons. *J. Neurosci.* **28,** 2874–2882
19. Koo, E. H., and Squazzo, S. L. (1994) Evidence that production and release of amyloid beta-protein involves the endocytic pathway. *J. Biol. Chem.* **269,** 17386–17389
20. Thinakaran, G., and Koo, E. H. (2008) Amyloid precursor protein trafficking, processing, and function. *J. Biol. Chem.* **283,** 29615–29619
21. Small, S. A., Kent, K., Pierce, A., Leung, C., Kang, M. S., Okada, H., Honig, L., Vonsattel, J. P., and Kim, T. W. (2005) Model-guided microarray implicates the retromer complex in Alzheimer's disease. *Ann. Neurol.* **58,** 909–919
22. Andersen, O. M., Reiche, J., Schmidt, V., Gotthardt, M., Spoelgen, R., Behlke, J., von Arnim, C. A., Breiderhoff, T., Jansen, P., Wu, X., Bales, K. R., Cappai, R., Masters, C. L., Gliemann, J., Mufson, E. J., Hyman, B. T., Paul, S. M., Nykjaer, A., and Willnow, T. E. (2005) Neuronal sorting protein-related receptor sorLA/LR11 regulates processing of the amyloid precursor protein. *Proc. Natl. Acad. Sci. U. S. A.* **102,** 13461–13466
23. Offe, K., Dodson, S. E., Shoemaker, J. T., Fritz, J. J., Gearing, M., Levey, A. I., and Lah, J. J. (2006) The lipoprotein receptor LR11 regulates amyloid beta production and amyloid precursor protein traffic in endosomal compartments. *J. Neurosci.* **26,** 1596–1603
24. Bertram, L., McQueen, M. B., Mullin, K., Blacker, D., and Tanzi, R. E. (2007) Systematic meta-analyses of Alzheimer disease genetic association studies: the AlzGene database. *Nat. Genet.* **39,** 17–23
25. Rogaeva, E., Meng, Y., Lee, J. H., Gu, Y., Kawarai, T., Zou, F., Katayama, T., Baldwin, C. T., Cheng, R., Hasegawa, H., Chen, F., Shibata, N., Lunetta, K. L., Pardossi-Piquard, R., Bohm, C., Wakutani, Y., Cupples, L. A., Cuenco, K. T., Green, R. C., Pinessi, L., Rainero, I., Sorbi, S., Bruni, A., Duara, R., Friedland, R. P., Inzelberg, R., Hampe, W., Bujo, H., Song, Y. Q., Andersen, O. M., Willnow, T. E., Graff-Radford, N., Petersen, R. C., Dickson, D., Der, S. D., Fraser, P. E., Schmitt-Ulms, G., Younkin, S., Mayeux, R., Farrer, L. A., and St. George-Hyslop, P. (2007) The neuronal sortilin-related receptor SORL1 is genetically associated with Alzheimer disease. *Nat. Genet.* **39,** 168–177
26. Tesco, G., Koh, Y. H., Kang, E. L., Cameron, A. N., Das, S., Sena-Esteves, M., Hiltunen, M., Yang, S. H., Zhong, Z., Shen, Y., Simpkins, J. W., and Tanzi, R. E. (2007) Depletion of GGA3 stabilizes BACE and enhances beta-secretase activity. *Neuron* **54,** 721–737
27. Landman, N., Jeong, S. Y., Shin, S. Y., Voronov, S. V., Serban, G., Kang, M. S., Park, M. K., Di Paolo, G., Chung, S., and Kim, T.-W. (2006) Presenilin mutations linked to familial Alzheimer's disease cause an imbalance in phosphatidylinositol 4,5-bisphosphate metabolism. *Proc. Natl. Acad. Sci. U. S. A.* **103,** 19524–19529
28. Puig, O., Caspary, F., Rigaut, G., Rutz, B., Bouveret, E., Bragado-Nilsson, E., Wilm, M., and Seraphin, B. (2001) The tandem affinity purification (TAP) method: a general procedure of protein complex purification. *Methods* **24,** 218–229
29. Vasilescu, J., Guo, X., and Kast, J. (2004) Identification of protein-protein interactions using in vivo cross-linking and mass spectrometry. *Proteomics* **4,** 3845–3854

30. Rigaut, G., Shevchenko, A., Rutz, B., Wilm, M., Mann, M., and Seraphin, B. (1999) A generic protein purification method for protein complex characterization and proteome exploration. *Nat. Biotechnol.* **17,** 1030–1032
31. Worby, C. A., and Dixon, J. E. (2002) Sorting out the cellular functions of sorting nexins. *Nat. Rev.* **3,** 919–931
32. Carlton, J., Bujny, M., Rutherford, A., and Cullen, P. (2005) Sorting nexins–unifying trends and new perspectives. *Traffic* **6,** 75–82
33. Seet, L. F., and Hong, W. (2006) The Phox (PX) domain proteins and membrane traffic. *Biochim. Biophys. Acta* **1761,** 878–896
34. Schöbel, S., Stephanie Neumann, S., Maren Hertweck, M., Bastian Dislich, B., Peer-Hendrik Kuhn, P.-H., Elisabeth Kremmer, E., Brian Seed, B., Ralf Baumeister, R., Christian Haass, C., and Stefan, F. Lichtenthaler, S. F. (2008) A novel sorting nexin modulates endocytic trafficking and α-secretase cleavage of the amyloid precursor protein. *J. Biol. Chem.* **283,** 14257–14268
35. Wassmer, T., Attar, N., Bujny, M. V., Oakley, J., Traer, C. J., and Cullen, P. J. (2007) A loss-of-function screen reveals SNX5 and SNX6 as potential components of the mammalian retromer. *J. Cell Sci.* **120,** 45–54
36. Lee, E. B., Skovronsky, D. M., Abtahian, F., Doms, R. W., and Lee, V. M. (2003) Secretion and intracellular generation of truncated Abeta in beta-site amyloid-beta precursor protein-cleaving enzyme expressing human neurons. *J. Biol. Chem.* **278,** 4458–4466
37. Bonifacino, J. S., and Hurley, J. H. (2008) Retromer. *Curr. Opin. Cell Biol.* **20,** 427–436
38. Carlton, J., Bujny, M., Peter, B. J., Oorschot, V. M., Rutherford, A., Mellor, H., Klumperman, J., McMahon, H. T., and Cullen, P. J. (2004) Sorting nexin-1 mediates tubular endosome-to-TGN transport through coincidence sensing of high- curvature membranes and 3-phosphoinositides. *Curr. Biol.* **14,** 1791–1800
39. Parks, W. T., Frank, D. B., Huff, C., Renfrew Haft, C., Martin, J., Meng, X., de Caestecker, M. P., McNally, J. G., Reddi, A., Taylor, S. I., Roberts, A. B., Wang, T., and Lechleider, R. J. (2001) Sorting nexin 6, a novel SNX, interacts with the transforming growth factor-beta family of receptor serine-threonine kinases. *J. Biol. Chem.* **276,** 19332–19339
40. Shiba, T., Kametaka, S., Kawasaki, M., Shibata, M., Waguri, S., Uchiyama, Y., and Wakatsuki, S. (2004) Insights into the phosphoregulation of beta-secretase sorting signal by the VHS domain of GGA1. *Traffic* **5,** 437–448
41. Spoelgen, R., von Arnim, C. A., Thomas, A. V., Peltan, I. D., Koker, M., Deng, A., Irizarry, M. C., Andersen, O. M., Willnow, T. E., and Hyman, B. T. (2006) Interaction of the cytosolic domains of sorLA/LR11 with the amyloid precursor protein (APP) and beta-secretase beta-site APP-cleaving enzyme. *J. Neurosci.* **26,** 418–428
42. Jacobsen, L., Madsen, P., Nielsen, M. S., Geraerts, W. P., Gliemann, J., Smit, A. B., and Petersen, C. M. (2002) The sorLA cytoplasmic domain interacts with GGA1 and -2 and defines minimum requirements for GGA binding. *FEBS Lett.* **511,** 155–158
43. Lee, J., Retamal, C., Cuitiño, L., Caruano-Yzermans, A., Shin, J. E., van Kerkhof, P., Marzolo, M. P., Bu, G. (2008) Adaptor protein sorting nexin 17 regulates amyloid precursor protein trafficking and processing in the early endosomes. *J. Biol. Chem.* **283,** 11501–11508
44. Fukumoto, H., Cheung, B. S., Hyman, B. T., and Irizarry, M. C. (2002) Beta-secretase protein and activity are increased in the neocortex in Alzheimer disease. *Arch. Neurol.* **59,** 1381–1389
45. Yang, L. B., Lindholm, K., Yan, R., Citron, M., Xia, W., Yang, X. L., Beach, T., Sue, L., Wong, P., Price, D., Li, R., and Shen, Y. (2003) Elevated beta-secretase expression and enzymatic activity detected in sporadic Alzheimer disease. *Nat. Med.* **9,** 3–4
46. Li, R., Lindholm, K., Yang, L. B., Yue, X., Citron, M., Yan, R., Beach, T., Sue, L., Sabbagh, M., Cai, H., Wong, P., Price, D., and Shen, Y. (2004) Amyloid beta peptide load is correlated with increased beta-secretase activity in sporadic Alzheimer's disease patients. *Proc. Natl. Acad. Sci. U. S. A.* **101,** 3632–3637
47. Velliquette, R. A., O'Connor, T., and Vassar, R. (2005) Energy inhibition elevates beta-secretase levels and activity and is potentially amyloidogenic in APP transgenic mice: possible early events in Alzheimer's disease pathogenesis. *J. Neurosci.* **25,** 10874–10883
48. Zhao, J., Fu, Y., Yasvoina, M., Shao, P., Hitt, B., O'Connor, T., Logan, S., Maus, E., Citron, M., Berry, R., Binder, L., and Vassar, R. (2007) Beta-site amyloid precursor protein cleaving enzyme 1 levels become elevated in neurons around amyloid plaques: implications for Alzheimer's disease pathogenesis. *J. Neurosci.* **27,** 3639–3649
49. Luo, Y., Bolon, B., Kahn, S., Bennett, B. D., Babu-Khan, S., Denis, P., Fan, W., Kha, H., Zhang, J., Gong, Y., Martin, L., Louis, J. C., Yan, Q., Richards, W. G., Citron, M., and Vassar, R. (2001) Mice deficient in BACE1, the Alzheimer's beta-secretase, have normal phenotype and abolished beta-amyloid generation. *Nat. Neurosci.* **4,** 231–232

Received for publication September 22, 2009.
Accepted for publication February 12, 2010.